



**HAL**  
open science

## Specific force map for smart machining applications with rotating tools

Sughosh Deshpande, Maria Clara Coimbra Gonçalves, Anna Carla Araujo,  
Pierre Lagarrigue, Yann Landon

### ► To cite this version:

Sughosh Deshpande, Maria Clara Coimbra Gonçalves, Anna Carla Araujo, Pierre Lagarrigue, Yann Landon. Specific force map for smart machining applications with rotating tools. Proceedings of the Institution of Mechanical Engineers, Part B: Journal of Engineering Manufacture, 2022, 10.1177/09544054221100320 . hal-03644109

**HAL Id: hal-03644109**

**<https://hal.science/hal-03644109>**

Submitted on 18 Apr 2022

**HAL** is a multi-disciplinary open access archive for the deposit and dissemination of scientific research documents, whether they are published or not. The documents may come from teaching and research institutions in France or abroad, or from public or private research centers.

L'archive ouverte pluridisciplinaire **HAL**, est destinée au dépôt et à la diffusion de documents scientifiques de niveau recherche, publiés ou non, émanant des établissements d'enseignement et de recherche français ou étrangers, des laboratoires publics ou privés.

## Specific force map for smart machining applications with rotating tools

Sughosh Deshpande<sup>1</sup>, Maria Clara Coimbra Gonçalves<sup>2</sup>, Anna  
Carla Araujo<sup>1, \*</sup>, Pierre Lagarrigue<sup>1</sup>, and Yann Landon<sup>1</sup>

<sup>1</sup>Institut Clément Ader, Université de Toulouse,  
CNRS/INSA/ISAE/Mines Albi/UPS, Toulouse, France

<sup>2</sup>USP - Universidade de São Paulo, São Paulo, Brazil

\*Corresponding author: Anna Carla Araujo,  
araujo@insa-toulouse.fr

April 16, 2022

### Abstract

Industry 4.0 is the need of the hour in current global market scenario and all the processes are moving towards automation and smart manufacturing. In machining, smart techniques implementation depends on developing a database for decision-making, which is the case for stack drilling in aerospace industry. In this application, choosing one optimal condition for several materials is a challenge due to their different machinability. Hence, material identification techniques are suitable approaches for adapting the cutting parameters in real time, which improves tool life, hole quality and productivity. In that regard, the goal of the present paper is to create a specific force data map for axial drilling and circular milling processes based on its experimental force and power measurements. To do that, experiments were separately carried out on Titanium and Aluminium workpieces in a range of cutting speed and feed conditions. The results show that specific cutting and feed forces for each material can be identified on distinct regions of the map, without thresholds overlapping. Given that, these maps can be used as a signature to distinguish two metallic materials in real time machining. In this case, the specific data points at the interface layers may offer advantage to accurately identify tool position unlike monitoring gradient of feed forces while drilling stacked materials. Therefore, smart machining techniques seeking cutting parameters optimization can be implemented for a particular material.

Keywords— Material identification, monitoring, helical milling, axial drilling, cutting forces, specific coefficients

## 1 Introduction

Multi stack drilling is one of the major operations in aircraft assemblies and it demands lots of time and resources to achieve high-quality holes. Usually, Titanium and Aluminium stacked materials are drilled before aircraft assembly and this poses a major challenge in machining due to the different materials' machinability. Some of the drilling challenges include poor finishing, burr formation and rapid tool wear [19]. These hole quality aspects, as exit burrs, can have a significant influence during assembly and affect productivity [6]. Hence, as thousands of holes have to be drilled for assembling an airplane, techniques considering different materials' machinability in a stack are crucial for performance maximization.

In this aspect, smart machining is a solution that refers to real time adaptation of cutting parameters for process optimization based in massive data from smart factories, specially using machine tool acquisition [10]. Previous research have presented prediction models and data monitoring techniques which can be helpful in smart machining applications. Wenkler et al. [17] developed a way of predicting specific cutting force by Artificial Neural Network which can be implemented in process planning or smart manufacturing. Hegab et al. [8] predicts tool wear by using Machine Learning models for a wide range of cutting conditions in drilling. Furthermore, a smart machining system is developed by monitoring spindle power and torque in order to optimize feed rates in milling by Park et al. [13].

One interest of applying smart machining during stack drilling is material identification. With this purpose, tool position detection inside the stacked layers is a key parameter so it is possible to adapt cutting parameters and machining strategies. Regarding this aspect, Pardo et al. [12] used cutting forces signals as input for three different decision-making algorithms to identify the tool position in stacked materials. Their objective was to compare the effectiveness of different approaches, which could be used for material identification. Jallageas et al. [9] developed a methodology to material identification in drilling multi-stacked material using thrust force signals. Their strategy used both: thresholds and gradient of forces to differentiate metallic materials and spectral analysis in order to distinguish aluminum and carbon fiber. The approach does not use any input process parameter, it uses pattern recognition for a specific drilling case. Material identification in stack drilling for a wide range of parameters is still a challenge that requires more research and the development. However, implementation of smart machining strategies in drilling alone may not completely optimize the process, so additionally other alternatives such as helical milling, also known as orbital drilling, can be applied.

Orbital drilling shows advantages regarding the process flexibility and ability to produce high-quality holes on different materials [14, 15]. Sun et al. [16] data shows that the fatigue life of holes produced by helical milling showed better life compared to conventional drilling. Although, cutting mechanistic is more complex in this process and so is the cutting models. Wu et al. [18] discussed force models for circular milling taking into account the uncut chip thickness

and feed rates variation at the corners. The cutting coefficients calculation in circular model can be further extended for helical milling adding vertical feed.

In both hole making processes of aerospace materials: axial drilling and helical milling, the specific cutting coefficients data can be used to identify the material being machined. They can act as material signatures to adapt proper cutting parameters in real time. These data could directly improve the process productivity and hole quality if appropriate cutting parameters are applied for the specific material.

Hence, the goal of this paper is to develop a data map of specific force coefficients related to each material for both process: axial drilling and circular milling processes, not developed in the previous papers, for further application in helical milling. The materials used for the experiments were aluminium 2017A and titanium Ti6Al4V, being subjected to a common set of cutting conditions. In the following sections, the force model and cutting coefficients are presented, as well the experimental set-up. The cutting forces and power results are presented and discussed, and lastly, the identification map with cutting coefficients for both processes is built.

## 2 Force model and specific force coefficients

Mechanistic force models can provide quantitative cutting force predictions based on the uncut chip thickness principle. Once experimental tests are made, the cutting force models enable estimating the specific cutting coefficients for a different set of variables, as describe by numerous papers [5, 1].

The forces for a general orthogonal cutting can be described by a mechanistic force model considering only cutting action of the cutting edge neglecting ploughing and chisel edge effects. The machining force  $\vec{F}_m$  is calculated considering the small finite elements of the cutting flute in the cutting edge referential frame decomposed: tangential ( $dF_c$ ), radial ( $dF_r$ ) and axial ( $dF_z$ ) components:

$$\vec{dF}_m = \begin{bmatrix} dF_c \\ dF_r \\ dF_z \end{bmatrix}. \quad (1)$$

The local force in point P of the cutting edge is a function of the uncut chip thickness  $h$  and the specific force coefficients:  $K_c$ ,  $K_r$  and  $K_z$ .

$$\begin{aligned} dF_c &= K_c(P).h(P)db \\ dF_r &= K_r(P).h(P)db \\ dF_z &= K_z(P).h(P)db \end{aligned}$$

where  $h(P)db$  is the elementary uncut chip load calculated on the reference point P in  $db$  elemental length of the cutting edge.

For each rotating tool machining process there are some assumptions in order to identify a global value for specific forces coefficient: in drilling, milling and circular milling, as follows.

## 2.1 Drilling

In drilling, local specific force coefficients can change along the cutting edge, as cutting speed varies from zero to the maximum cutting speed  $V_c$  on the tool nominal radius  $D/2$ . Also, cutting angles can change along the edge. Although, for a fixed tool geometry, it is possible to calculate an average specific force coefficient along the edge. It can be calculated using the total chip load per cutting edge  $A_c = \int hdb = f_z(D/2) = \frac{f}{2}(D/2)$  (where  $f$  is the feed per revolution for a 2 flutes tool and  $f_z$  is the feed per tooth).

In drilling, it is not possible to experimentally measure the cutting force for a single cutting edge  $F_c$  (N), because both edges are in contact with the workpiece and they have opposite directions. The average specific cutting force  $K_c$  (N/mm<sup>2</sup>) for a tool-workpiece pair in drilling is calculated using the experimental cutting power  $P_c$ , contribution of both cutting edges [17]:

$$K_c = \frac{F_c}{A_c} = \frac{120 P_c}{V_c f_z D} \quad (2)$$

On other hand, it is possible to measure the feed force  $F_z$  and to directly calculate the feed force  $F_f$  for each cutting edge ( $F_z = 2F_f$ ). The specific feed force  $K_f$  (MPa) is calculated as:

$$K_f = \frac{F_f}{A_c} = \frac{F_f}{f_z (D/2)} = \frac{F_z}{f_z D} \quad (3)$$

## 2.2 Milling

In milling, in order to determine the cutting coefficients of the tool-workpiece pair, the local cutting force  $dF_c(t)$  and the radial force  $dF_r(t)$  are analyzed considering the variation of the uncut chip thickness along the tool rotation. Martellotti equation [4] described  $h(\theta_2)$  as a function of the tool rotation angle  $\theta_2$ . The forces in axial direction ( $dF_z$ ) can be neglected, if the helix angle is small.

When summing the contributions of each cutting part  $db$ ,  $dF_c(t)$  and  $dF_r(t)$ , the directions are not the same and a change to a fixed referential is necessary. From there,  $dF_x(t)$  and  $dF_y(t)$  can be calculated and the machining tool for each cutting edge in contact to the workpiece at the time  $t$  can be calculated.

As in drilling, some assumptions should be made for the identification of specific cutting force and specific radial force. It is considered that the maximum force is achieved in the position of  $\theta_2$  when the average uncut chip thickness along the cutting edge is higher. The reference frame is now fixed in the rotating tool  $\theta_2$  and not in each element. Then, the approximation done lead to:

$$K_c = \frac{F_c(\theta_2)}{A_c(\theta_2)} \longrightarrow K_c = \frac{F_c(max)}{A_c(max)} \approx \frac{F_c(max)}{h'(max).a_p} \quad (4)$$

$$K_r = \frac{F_r(\theta_2)}{A_c(\theta_2)} \longrightarrow K_r = \frac{F_r(max)}{A_c(max)} \approx \frac{F_r(max)}{h'(max).a_p} \quad (5)$$

Considering that the measurement is taken using a fixed dynamometer, the acquisition is done in a  $XY$  fixed referential frame. In linear milling, when feed direction is aligned with X direction :

$$\begin{bmatrix} F_X \\ F_Y \end{bmatrix} = \begin{bmatrix} \sin(-\theta_2) & -\cos(-\theta_2) \\ \cos(-\theta_2) & \sin(-\theta_2) \end{bmatrix} \cdot \begin{bmatrix} F_c(\theta_2) \\ F_r(\theta_2) \end{bmatrix} \quad (6)$$

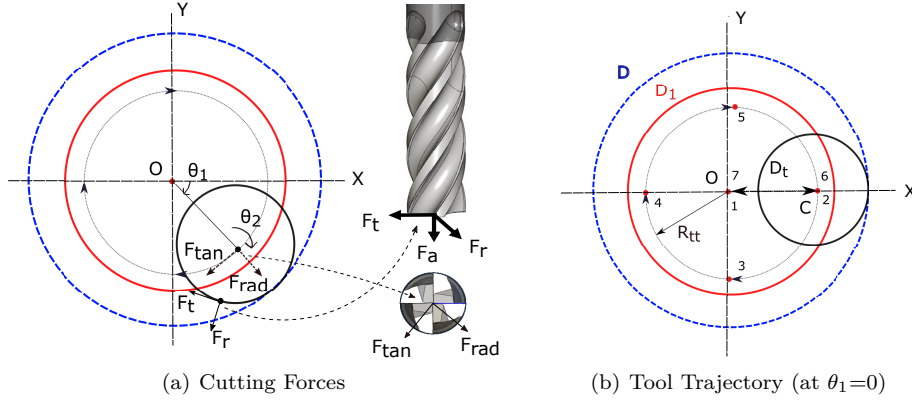


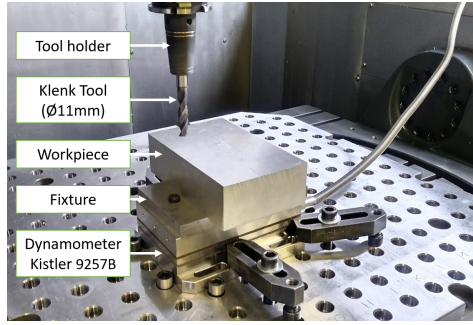
Figure 1: Referential Frames in X and Y indicating cutting forces and tool trajectory in circular milling

### 2.3 Circular Milling

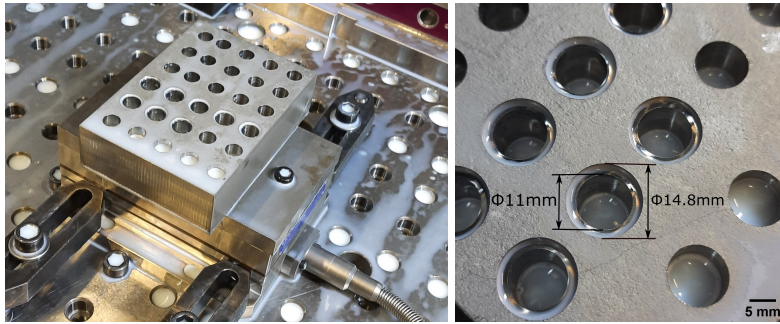
Unlike in linear milling, circular milling involves movement of tool around a centered fixed point in clockwise or anticlockwise direction to enlarge a existing hole diameter. Figure 1(b) shows the circular milling tool trajectory (at  $\theta_1=0$ ) and the associated geometric parameters. A tool of diameter  $D_t$  with center  $C$  is moving around the hole center  $O$ .  $D_1$  refers to pre hole diameter and  $D$  is the final diameter to be achieved after circular milling.  $R_{tt}$  is the tool trajectory radius with reference to hole center  $O$  [3].

In circular milling, cutting forces at the cutting edge have different referential frames that have to be analyzed in order to determine the cutting coefficients of the tool-workpiece pair. The cutting forces exerted by the tool on the workpiece can be seen in Figure 1(a). Feed motion produces  $F_{tan}$  and  $F_{rad}$  forces and the cutting action gives rise to tangential ( $F_t$ ), radial ( $F_r$ ) and axial forces ( $F_z$ ) at the cutting edge. It can be noted that the direction of feed forces in circular milling changes continuously unlike in linear milling where feed direction and feed force direction remain unchanged. In circular milling context, forces in axial direction ( $F_z$ ) can be neglected.

The forces measured during experiments by the dynamometer are in  $XY$  referential frame:  $F_X$  and  $F_Y$  as shown in Figure 1(a). The tool rotates around



(a) Experimental elements



(b) Workpiece (Titanium)

(c) Milled dimensions (Titanium)

Figure 2: Experimental setup

the hole center  $O$  in clockwise direction given by angular position  $\theta_1$  and around its own axis given by  $\theta_2$ , also in clockwise direction. The forces  $F_X$  and  $F_Y$  can be transformed using a rotation matrix (Eq. 7) to deduce  $F_{tan}$  and  $F_{rad}$  at the tool center.  $F_{tan}$  and  $F_{rad}$  are significant to understand tool deflection effects on hole quality. To calculate  $F_t$  and  $F_r$  at the cutting edge, the rotation matrix as a function of  $\theta_2$  and the dynamometer referential frame components ( $F_X$  and  $F_Y$ ) (Eq. 8) can be applied. The specific cutting coefficients  $K_c$  and  $K_r$  ( $N/mm^2$ ) are identified by analyzing  $F_t$  and  $F_r$  maximum values for a particular set of tool revolutions using Eq.4 and Eq.5.

$$\begin{bmatrix} F_{rad} \\ F_{tan} \end{bmatrix} = \begin{bmatrix} \cos(-\theta_1) & -\sin(-\theta_1) \\ \sin(-\theta_1) & -\cos(-\theta_1) \end{bmatrix} \cdot \begin{bmatrix} F_X \\ F_Y \end{bmatrix} \quad (7)$$

$$\begin{bmatrix} F_t(\theta_2) \\ F_r(\theta_2) \end{bmatrix} = \begin{bmatrix} -\sin(-\theta_2) & -\cos(-\theta_2) \\ -\cos(-\theta_2) & -\sin(-\theta_2) \end{bmatrix} \cdot \begin{bmatrix} F_X \\ F_Y \end{bmatrix} \quad (8)$$

### 3 Materials and methods

In this section, drilling and circular milling experiments are presented in Aluminium (2017A) alloy and Titanium (Ti6Al4V) alloy workpieces measuring cutting forces and cutting power. The experiments were carried out for a specific range of cutting conditions, following the experimental setup and the design of experiments described below.

Table 1: Design of Experiments: Cutting conditions

Operation	Workpiece	Cutting speed (m/min)	Feed (mm/th)
Drilling ( $\varnothing 11$ mm, 2 flutes)	Aluminium	20 / 60 / 100	0.02 / 0.10 / 0.18
	Titanium	20 / 40 / 60	0.02 / 0.06 / 0.10
Milling ( $\varnothing 8$ mm, 4 flutes, $30^\circ$ helix)	Aluminium	40	0.02 / 0.10 / 0.18
	Titanium	40	0.02 / 0.10 / 0.18

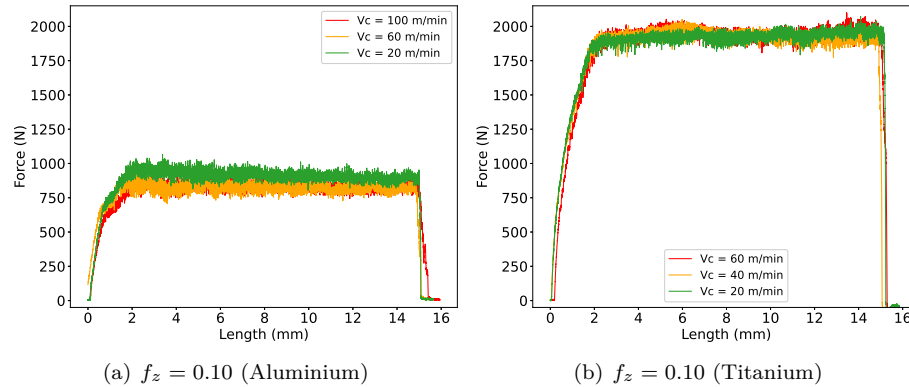


Figure 3: Experimental feed force for drilling Aluminium and Titanium

#### 3.1 Experimental setup

All drilling and milling experiments were carried out on a CNC milling center DMU85-DMG mono block machine. Flood water-based through coolant was used for drilling and circular milling was carried out in dry condition. The tools used for the experiments were: carbide drills from Klenk having diameter 11 mm, one of the most commonly used in aerospace stack drilling applications, and carbide end mills of 8 mm diameter from Fraisa.

The workpieces were fixed on a 9257B Kistler dynamometer, as shown in Figure 2(a), using only its internal measuring region, connected to a 5070 Kistler

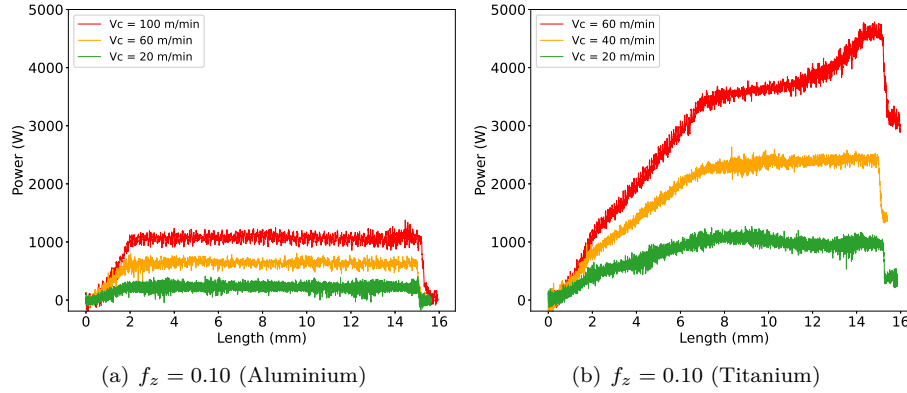


Figure 4: Experimental cutting power for drilling Aluminium and Titanium

amplifier. For power acquisition, a Montronix power sensor PS200-DGM measured the input of effective electrical power of the spindle.

Analogical data of force and power were converted to digital using a 9201 National Instruments acquisition module with 10 kHz acquisition rate. The measured forces were filtered using a low pass Butter-worth filter with cutoff frequency of 700 Hz (appropriated to the maximum spindle speed).

### 3.2 Design of Experiments

Table 1 summarizes the cutting conditions on Aluminium and Titanium along with tool details for drilling and circular milling operations. The range of cutting parameters is wider than usual because the goal was to compare the machining responses in both materials and processes for a wide range of cutting conditions. The lowest feed per tooth allowed for a monoblock carbide tool is included ( $0.02\text{mm/tooth}$ ) in the parameters range. Drilling depth was set as  $15\text{mm}$  in case of axial drilling for both materials. Circular milling was carried out on the drilled hole with an axial depth of  $1\text{mm}$  and a radial width of cut of  $1.9\text{mm}$ . In order to have a cutting continuity coefficient  $c$  less than 1, in other words to have only one cutting flute in contact with the workpiece at any point of time [2], the chosen final milled hole diameter is  $14.8\text{mm}$ .

## 4 Experimental results

The following subsections present the results of feed force and power for drilling along with cutting forces for circular milling. The graphs are presented in terms of length of the hole for drilling for various cutting speeds and feed rates. Circular milling forces are presented in terms of tool angular position  $\theta_1$  (around O) which is taken as a reference for all the feed rates and cutting speed values

tested. It should be noted that the trajectory rate ( $\theta_1/time$ ) changes based on variation in feed rate values.

#### 4.1 Feed force and power in drilling

Regarding the cutting force, Figure 3 shows the results obtained per depth of the hole for Aluminium and Titanium respectively. Each figure contains results of different cutting speeds obtained at  $f_z=0.1$  mm/th. Varying cutting speeds do not greatly differ the feed force values as seen in the Figure 3. Also, the region where the tip of the tool starts entering the workpiece is clearly observed from the increasing force slope, then the cut is stabilized. The complete graphical results from the experiment for other feed values are referred in the earlier article from Gonçalves et al. [7].

Cutting power results are shown in Figure 4 for Aluminium and Titanium at  $f_z=0.1$  mm/th. For Titanium, there is an increase in power when the tool penetrates the workpiece unlike Aluminium which remains almost stable during drilling. This can be attributed to the elastic recovery of material, since no tool conicity was observed. An important fact that can be observed comparing both graphs is: the results are the same during the first 2 mm penetration for both materials, when only the chisel point is in contact with the workpiece. In consequence, identifying the materials during this phase of drilling, and also in the transition of materials, is challenging in stack drilling. This was also observed previously by Pardo et al. [12].

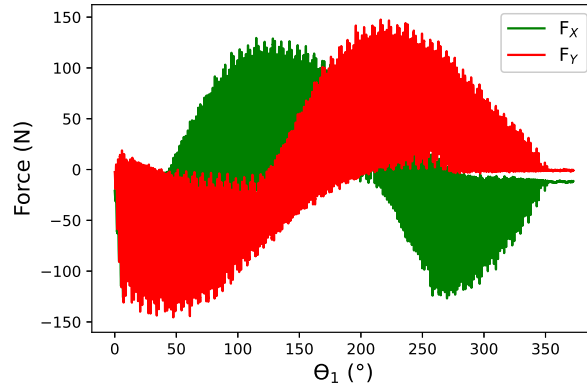


Figure 5: Experimental forces  $F_X$  and  $F_Y$  during Circular Milling of Aluminium as an example ( $f_z=0.1$  mm/th and  $V_c=40$ m/min)

#### 4.2 Forces in Circular Milling

The cutting forces  $F_X$  and  $F_Y$  obtained with the dynamometer during circular milling can be seen in the Figure 5. The graph shows the variation of forces

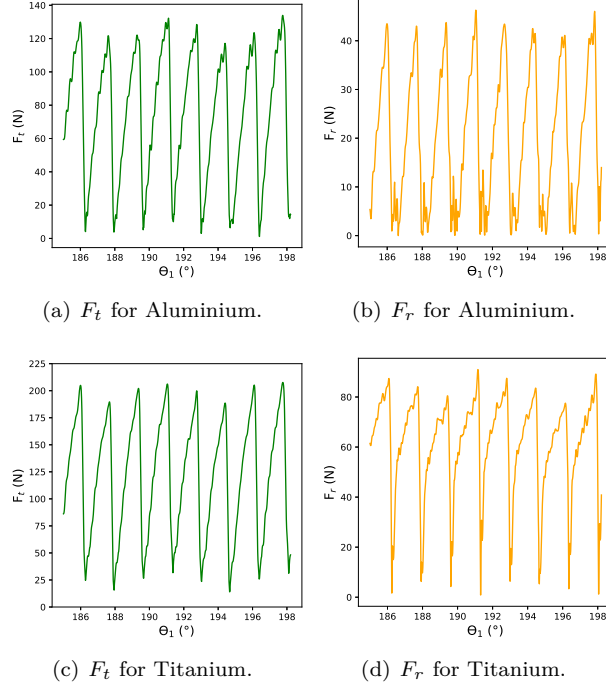


Figure 6: Calculated  $F_t$  and  $F_r$  during 2 revolutions in circular milling of Aluminium and Titanium (window on  $\theta_1 = [185^\circ - 198^\circ]$ ) at  $f_z = 0.1$  mm/th and  $V_c = 40$  m/min

with reference to dynamometer X and Y direction during the tool trajectory as a function of  $\theta_1$  in clockwise direction.

Figure 6 shows the variation of transformed forces at the cutting edge ( $F_t$  and  $F_r$ ) in a time window of two tool revolutions  $\theta_2 = [0 - 720^\circ]$  in Aluminium and Titanium at  $f_z = 0.1$  mm/th and  $V_c = 40$  m/min. Eight peaks can be observed in the transformed forces for a 4 flutes end mill. The cutting forces were transformed as previously indicated in Eq. 8.

## 5 Experimental specific force coefficients

After acquiring forces and power data for the analyzed processes, the specific cutting force coefficients were estimated. They are presented in the following subsections for the drilling and milling operations, followed by the targeted identification map. It is important to claim that the circular milling experiments were done after the analysis of drilling experiments. As the aim of this paper is the material identification based on the data, the range of feed per tooth was

narrowed to 0.10 and 0.18 mm/th, where the values of forces were closer. Also, low feed rate values as 0.02 mm/tooth are very rarely used in the industry for these materials.

### 5.1 Specific force coefficients in drilling

The  $K_c$  and  $K_f$  values for different feed rates are shown in Figure 7(a) and 7(b), where comparisons between both materials are made. The behavior of results are similar, considering that the values for Titanium are higher due to its poorest machinability.  $K_c$  and  $K_f$  values are calculated as indicated in the Eq.2 and 3 previously.

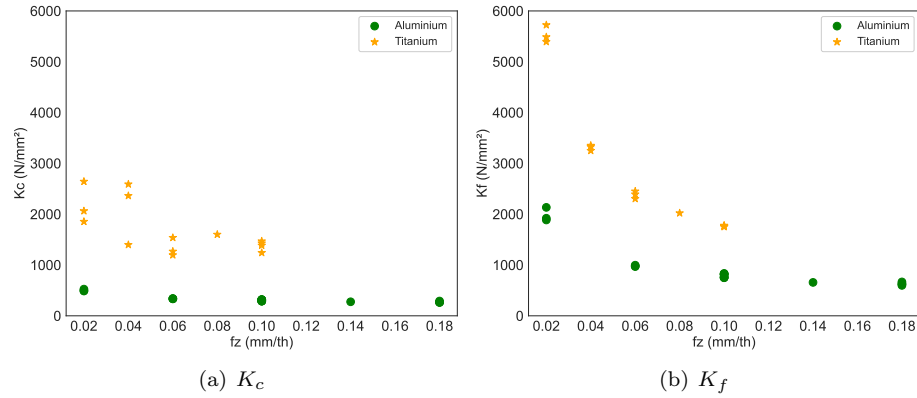


Figure 7: Specific force coefficients ( $K_c$  and  $K_f$ ) for Aluminium and Titanium in drilling

### 5.2 Specific force coefficients in circular milling

Figure 8(a) and 8(b) shows  $K_c$  and  $K_r$  values against feed for Aluminium and Titanium. They were calculated using  $F_t$  and  $F_r$  values, respectively, for a specific set of tool revolutions.

The data includes values calculated at several tool angle positions  $\theta_1$  for each specific feed rate and cutting velocity with the objective of having a representative value with larger spectrum of experimental variability and noise.

It can be noted in Figure 8 that the specific coefficient values for Titanium are considerably higher compared to Aluminium, as observed for drilling.

### 5.3 Identification map

In this article we propose a clear distinction between both materials and force coefficient values identified in a single graphic, so called identification map.

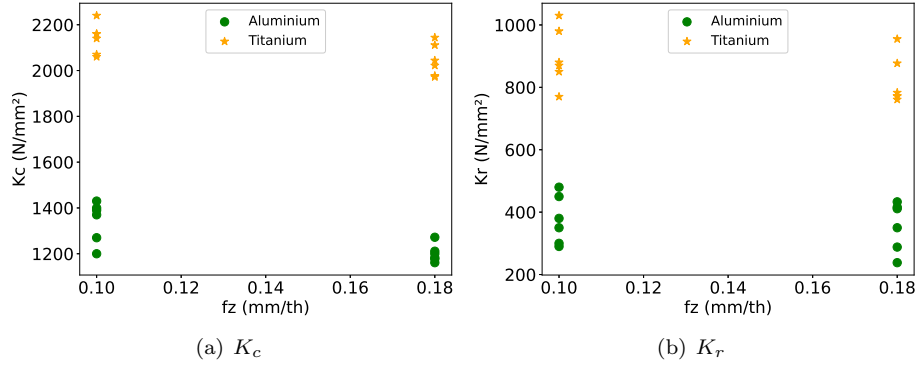


Figure 8: Specific force coefficients ( $K_c$  and  $K_r$ ) for Aluminium and Titanium in circular milling

Even though the analysis of force coefficients per feed shows distinct results for different materials, identification can be mistaken through these results. This is because of the possibility of having similar coefficient values for both the materials at different feed rates.

Figures 9(a) and 9(b) presents the identification map using  $K_c$  per  $K_f$  for drilling and  $K_c$  per  $K_r$  for circular milling. It should be noted that in drilling  $K_f$  is derived from the feed force and in circular milling  $K_r$  is derived from the radial cutting force. The areas identified as Aluminium and Titanium are clusters with a simple method using minimum and maximum points on the map, without thresholds overlap. Although, the methodology could be improved using other sophisticated clustering methods. This clear distinction increases the material identification precision, which is the first step of self-adjustment techniques (changing spindle speed or feed per tooth).

In extreme situations, the acquired machining data can be incorporated to the commercial software in to alarm or stop the tool rotation in extreme situations, as it is already the case of power [11].

## 6 Conclusions

The main focus of this article was to demonstrate the possibility of material identification during hole making operations of two different materials by analyzing specific force coefficients. In this regard, cutting force and power data were analyzed to identify specific force coefficients for Titanium and Aluminium. Our work proposes utilisation of data points of specific force coefficients for material identification while drilling stacked materials. This novel technique can help to adapt proper cutting parameters in real time. Such data maps with precise points of specific force coefficients can have advantages over monitoring of thrust forces for gradient change to identify materials or tool position in the

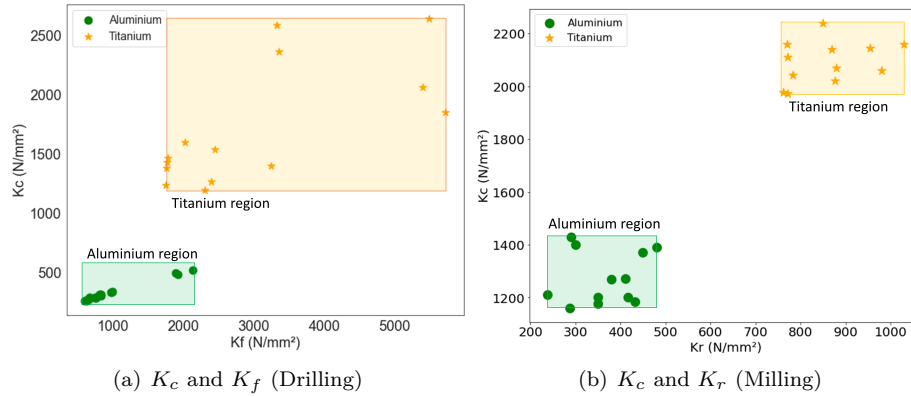


Figure 9: Identification Map for Drilling and Circular Milling in Aluminium and Titanium

stack.

The results can be summarized as follows:

- In both operations, specific force coefficients are identified in different regions of the map for Titanium and Aluminium due to the materials distinct machinability;
- During initial phase of axial drilling, when only chisel point is inside the material, the signals are similar comparing both materials and difficult to identify;
- Considering drilling results in Titanium, the elastic recovery of material leads to an increase in power when the tool penetrates the workpiece. This elastic recovery disturbs the identification, it could lead to wrong interpretation of increasing specific cutting force inside the hole, which is not the case.
- In circular milling, the transformed feed forces ( $F_{tan}$  and  $F_{rad}$ ) can be further analyzed to understand its relation with respect to hole quality and attributed to optimal cutting conditions for a tool-material pair.
- The variation of  $K_r$  values in circular milling compared to  $K_c$  values for a particular feed and velocity may be attributed to tool deflection/vibrations which is also reflected in radial forces. However, there is a distinct separation when the values are compared with both materials.

Hence, the gap between the cutting force coefficients for both materials makes it suitable for applying smart machining techniques using data monitoring in hole making processes of stacked materials made out of Aluminium and Titanium.

Thus, as shown in this work, the specific force coefficients makes it possible to clearly identify different materials in real time, which is calculated by online monitoring of cutting forces and power. The calculation of instantaneous specific force coefficients for material identification and real time decision making to adapt cutting parameters will optimise the hole making process.

## References

- [1] Y Altintas. Manufacturing Automation: Metal Cutting Mechanics, Machine Tool Vibrations, and CNC Design. *Applied Mechanics Reviews*, 54(5):B84–B84, 09 2001.
- [2] Anna Carla Araujo and Guillaume Fromentin. Modeling thread milling forces in mini-hole in dental metallic materials. *Procedia CIRP*, 58:623–628, 2017.
- [3] Anna Carla Araujo, Guillaume Fromentin, and Gerard Poulachon. Analytical and experimental investigations on thread milling forces in titanium alloy. *International Journal of Machine Tools and Manufacture*, 67:28–34, 2013.
- [4] Anna Carla Araujo, Jose Luis Silveira, Martin B.G. Jun, Shiv G. Kapoor, and Richard DeVor. A model for thread milling cutting forces. *International Journal of Machine Tools and Manufacture*, 46(15):2057–2065, 2006.
- [5] E. J. A. Armarego and N. P. Deshpande. Computerized Predictive Cutting Models for Forces in End-Milling Including Eccentricity Effects. *CIRP Annals*, 38(1):45–49, January 1989.
- [6] L K Gillespie. Burrs produced by drilling. Technical report, The Bendix Coporation, 8 1976.
- [7] Maria Clara Coimbra Gonçalves, Gilmar Ferreira Batalha, Yann Landon, and Anna Carla Araujo. Smart drilling: material identification using specific force map. In 11<sup>o</sup> COBEF, pages 1–7, Curitiba, Brazil, May 2021.
- [8] H. Hegab, M. Hassan, S. Rawat, A. Sadek, and H. Attia. A smart tool wear prediction model in drilling of woven composites. *The International Journal of Advanced Manufacturing Technology*, 110(11):2881–2892, 2020.
- [9] Jeremy Jallageas, Matthieu Ayfre, Mehdi Cherif, Jean-Yves K’nevez, and Olivier Cahuc. Self-adjusting cutting parameter technique for drilling multi-stacked material. *International Journal of Materials and Manufacturing*, 9(1):24–30, 2015. Publisher: SAE International.
- [10] Chuipin Kong, Wei Liu, Xionghui Zhou, Qiang Niu, and Jingguo Jiang. A study on a general cyber machine tools monitoring system in smart factories. *Proceedings of the Institution of Mechanical Engineers, Part B: Journal of Engineering Manufacture*, 235(14):2250–2261, 2021.

- [11] L. Köttner, J. Mehnen, D. Romanenko, S. Bender, and W. Hintze. Process monitoring using machine learning for semi-automatic drilling of rivet holes in the aerospace industry. In Bernd-Arno Behrens, Alexander Brosius, Wolfgang Hintze, Steffen Ihlenfeldt, and Jens Peter Wulfsberg, editors, *Production at the leading edge of technology, Lecture Notes in Production Engineering*, pages 497–507. Springer, 2021.
- [12] Andrea Pardo, Robert Heinemann, Nuno Miguel Nobre, and Luke Bagshaw. Assessment of decision-making algorithms for adaptive drilling of aerospace stacks. *Procedia CIRP*, 99, January 2021.
- [13] Hong-seok Park, Bowen Qi, Duck-Viet Dang, and Dae Yu Park. Development of smart machining system for optimizing feedrates to minimize machining time. *Journal of Computational Design and Engineering*, 5(3):299–304, 2018.
- [14] Robson Bruno Dutra Pereira, Lincoln Cardoso Brandão, Anderson Paulo de Paiva, João Roberto Ferreira, and J. Paulo Davim. A review of helical milling process. *International Journal of Machine Tools and Manufacture*, 120:27–48, September 2017.
- [15] Francisco Puerta Morales, Jorge Gómez, and Severo Raul Fernandez Vidal. Study of the Influence of Helical Milling Parameters on the Quality of Holes in the UNS R56400 Alloy. *Applied Sciences*, 10:845, January 2020.
- [16] D. Sun, Patrick Lemoine, Daniel Keys, Patrick Doyle, Savko Malinov, Qing Zhao, Xuda Qin, and Yan Jin. Hole-making processes and their impacts on the microstructure and fatigue response of aircraft alloys. *The International Journal of Advanced Manufacturing Technology*, 94, February 2018.
- [17] Eric Wenkler, Frank Arnold, Albrecht Hänel, Andreas Nestler, and Alexander Brosius. Intelligent characteristic value determination for cutting processes based on machine learning. *Procedia CIRP*, 79:9–14, January 2019.
- [18] Baohai Wu, Xue Yan, Ming Luo, and Ge Gao. Cutting force prediction for circular end milling process. *Chinese Journal of Aeronautics*, 26(4):1057–1063, August 2013.
- [19] Zhaoju Zhu, Kai Guo, Jie Sun, Jianfeng Li, Yang Liu, Yihao Zheng, and Lei Chen. Evaluation of novel tool geometries in dry drilling aluminium 2024-T351/titanium Ti6Al4V stack. *Journal of Materials Processing Technology*, 259:270–281, September 2018.